Taylor & Francis
Taylor & Francis Group

BRIEF COMMUNICATION

🔓 OPEN ACCESS Check for updates

Functional sequestration of microRNA-122 from Hepatitis C Virus by circular RNA sponges

Isabelle Jost[a,†], Lyudmila A. Shalamova[a,b,†], Gesche K. Gerresheim[a,b], Michael Niepmann[b], Albrecht Bindereif [ID][a] and Oliver Rossbach[a]

[a]Institute of Biochemistry, Faculty of Biology and Chemistry, University of Giessen, Heinrich-Buff-Ring 17, Giessen, Germany; [b]Institute of Biochemistry, Faculty of Medicine, University of Giessen, Friedrichstrasse 24, Giessen, Germany

ABSTRACT

Circular RNAs (circRNAs) were recently described as a novel class of cellular RNAs. Two circRNAs were reported to function as molecular sponges, sequestering specific microRNAs, thereby de-repressing target mRNAs. Due to their elevated stability in comparison to linear RNA, circRNAs may be an interesting tool in molecular medicine and biology. In this study, we provide a proof-of-principle that circRNAs can be engineered as microRNA sponges. As a model system, we used the Hepatitis C Virus (HCV), which requires cellular microRNA-122 for its life cycle. We produced artificial circRNA sponges *in vitro* that efficiently sequester microRNA-122, thereby inhibiting viral protein production in an HCV cell culture system. These circRNAs are more stable than their linear counterparts, and localize both to the cytoplasm and to the nucleus, opening up a wide range of potential applications.

Circular RNAs (circRNAs) have recently been discovered as a large class of ubiquitously expressed, tissue-specific, mainly noncoding RNA [1,2]. They are produced by the canonical splicing machinery by a process termed "back-splicing", where a donor splice site is spliced to an upstream instead of a downstream acceptor site [3]. They are mostly located in the cytoplasm and appear to be generally more stable than linear RNA due to their resistance to exonucleolytic degradation [2]. The first described function for cellular circRNAs was serving as microRNA (miRNA) sponges. Two circRNAs, CDR1as/ciRS-7 and SRY, were found to contain highly conserved binding sites for miRNA-7 or miRNA-138, respectively [4,5]. CDR1as/ciRS-7 is highly expressed in brain and functionally suppresses miRNA-7 activity, thereby de-repressing natural miRNA-7 targets. Recently it was shown that CDR1as/ciRS-7 is essential for normal brain function, and knockout caused dysfunctional synaptic transmission in mice [6].

In this study, we aim to provide a proof-of-principle that artificial circRNAs can be engineered as custom miRNA sponges to sequester miRNAs relevant in human disease. As a model system, we chose the Hepatitis C Virus (HCV), a positive-sense single-stranded RNA virus that lacks a 5′-cap structure and initiates its translation via a highly structured internal ribosome entry site (IRES). The virus is hepatocyte-specific, partly due to its dependence on the host miRNA-122 that is exceptionally abundant in hepatocytes [7]. miRNA-122 binds to two distinct binding sites

at the very 5′-end of the virus genome, where it protects the virus RNA from exonucleolytic degradation by Xrn-1, enhances viral replication and translation from the viral IRES-element, consequently facilitating propagation of HCV [8–11].

miRNA-122 was therefore already utilized as a drug target in anti-HCV therapy. The first antimiR-drug Miravirsen was successfully tested in phase II clinical trials [12]. Miravirsen is a locked-nucleic-acid (LNA)/DNA-mixmer oligonucleotide that is complementary to miRNA-122, and tightly binds and functionally sequesters the miRNA [13]. In patients, virus titers were decreased to non-detectable levels after four weeks of subcutaneous administration [12]. Recently a second anti-miRNA-122 drug was clinically tested. RG-101, an N-acetylgalactosamine-conjugated anti-miRNA-122 oligonucleotide substantially reduced viral load in combination with direct-acting antiviral drugs [14].

Here we show that artificial circRNAs can be engineered to contain an array of miRNA-122 binding sites, and produced by *in vitro* transcription and circularization. We provide evidence that highly complementary binding sites are suitable to tightly bind and sequester the cellular miRNA-122 *in vitro* and *in vivo*. These artificial miRNA-sponges are more stable than their linear counterparts when transfected in cells. Ultimately, they sequester miRNA-122 from HCV in two reporter systems, including a full-length infectious HCV cell culture system. Viral protein production is strongly reduced, with comparable efficiency as Miravirsen. Interestingly, these artificial circRNA

sponges localize both to the cytoplasm and to the nucleus, making them an interesting tool for applications in molecular medicine and biology.

To achieve a functional sequestration of miRNA-122 from HCV, a molecular sponge needs to compete with the viral binding sites. These reside at the 5′-end of the HCV plus strand RNA genome and follow the canonical principles of miRNA-mRNA interactions (Fig. S1A) [8,10,11]. To design a molecular sponge, three different miRNA-122 binding sites were analyzed: an experimentally validated endogenous binding site from the *IGF1R* mRNA 3′-UTR [15], a bulged binding site lacking complementarity at nucleotides 10–12 and a perfectly complementary binding site, which is thought to be cleaved by the miRNA-122-RISC complex (Fig. 1A) [16,17]. Four copies of these binding sites, corresponding seed mutant versions (Fig. 1A) and unrelated 3′-UTRs without miRNA-122 binding sites (derived from *LAPTM4A*, *HNRNPK* and *KPNB1* mRNAs) were inserted into the firefly luciferase reporter 3′-UTR of a dual-luciferase reporter system. The reporter constructs were transfected into HuH-7.5 cells that express high levels of miRNA-122, and luciferase activity was monitored in cell lysates. The *IGF1R* binding sites did not repress luciferase expression, whereas the wildtype bulged and both perfectly complementary sites did (Fig. 1B). In the latter, the seed mutation is not sufficient to completely abolish repression of luciferase expression. The reduced luciferase activity may not only be due to translational repression but also cleavage and/or destabilization of the luciferase reporter RNA as apparent from semiquantitative RT-PCR analysis (Fig. 1C).

Moreover, we used a direct biochemical approach to verify interaction of miRNA-122 with the binding sites. Biotinylated *in vitro* transcripts carrying the same sequences as

the luciferase reporters were incubated in HuH-7 cytoplasmic extract, and bound miRNA-122 was analyzed by northern blot. Both the bulged and perfectly complementary binding sites efficiently pulled down miRNA-122, in contrast to the *IGF1R*-derived site or the corresponding seed mutants (Fig. 1D). Surprisingly, we did not observe cleavage of the perfectly complementary binding site under these conditions (Fig. 1D, lower panel).

The two naturally occurring circular RNA sponges ciRS-7/CDR1as and SRY have 73 and 16 consecutive miRNA binding sites, respectively [4,5]. Repetitive elements as the artificial binding sites tested in Fig. 1 are likely to complicate standard molecular techniques as PCR, cloning, or Sanger sequencing. For this reason the binding sites used in the following are limited to 8-mers, including 4 nucleotides (nt) spacer sequences, resulting in optimal spacing of 20 nt between adjacent seed sites. Analyses of endogenous miRNA-binding sites showed that a spacing of 16–20 nt between seed binding sites is overrepresented, and allows efficient binding of multiple miRNA/Ago2 complexes [17]. To enhance RNA circularization *in vitro* and to overcome the disadvantageous repetitive nature of the constructs used, a reverse complementary repeat of 11 nt was added to both ends of the transcript, resulting in a 11 bp stem with an open loop structure of 10 nt (Fig. 2A). A 63 nt constant region between this stem and the sponge sequence allows detection of all constructs using the same PCR primers or northern hybridization probes. Efficient circularization of *in vitro* transcripts is achieved by an optimized *in vitro* circularization protocol using T4 RNA ligase 1. This procedure results in circular RNA or linear dimers (Fig. 2B), which can be distinguished by the differential migration behavior of circular RNA in denaturing gels of varying polyacrylamide concentration [19] (Fig. 2C). Since the control 3′-
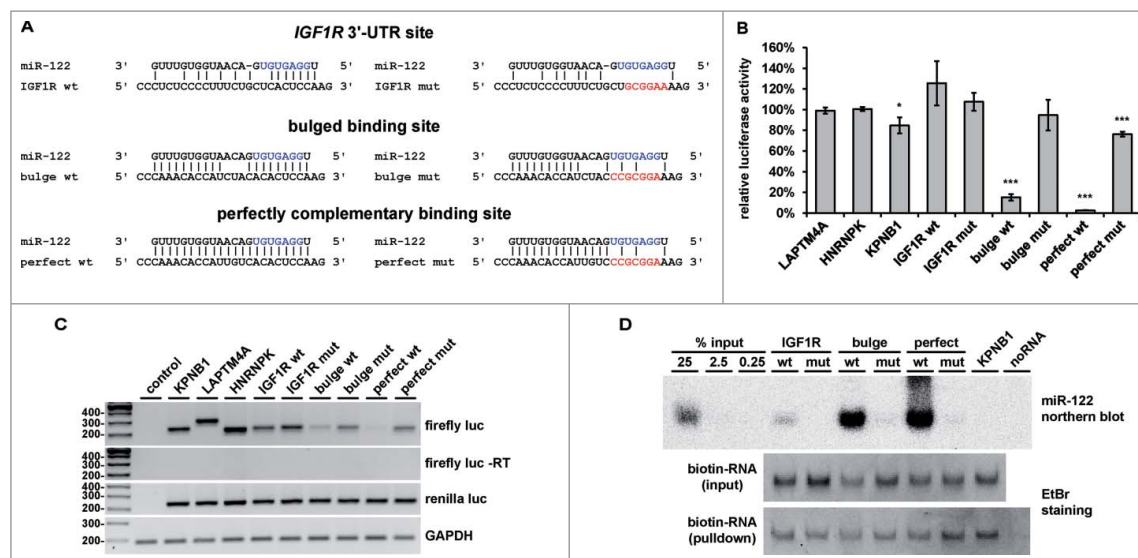

Figure 1. Characterization of miRNA-122 binding sites. (A) Representation of the miRNA-122 wildtype binding sites (wt, left) used in this study as well as the corresponding seed mutants (mut, right). (B) Dual luciferase reporter assay using four copies of the binding sites shown in (A) inserted into the 3′-UTR of a firefly luciferase reporter. *LAPTM4A*, *HNRNPK* and *KPNB1* 3′-UTR fragments of similar length without miRNA-122 binding sites served as controls. Firefly luciferase activity was normalized to a renilla luciferase reporter encoded by the same plasmid and to *LAPTM4A* control. Error bars represent s.d. (n = 3). *$P < 0.05$; ***$P < 0.001$. (C) RT-PCR of the reporter RNAs from (B). Firefly and renilla luciferase RNA were detected, as well as cellular GAPDH mRNA. As a control for the absence of plasmid DNA, an experiment without reverse transcriptase was used (firefly luc -RT). (D) Neutravidin-biotin pulldown from HuH-7 cytoplasmic extracts using *in vitro* transcribed and biotinylated RNA carrying four copies of the binding sites displayed in (A) or *KPNB1* 3′-UTR fragment of the same length. Precipitated miRNA-122 was detected by northern blot. Input and bound biotinylated RNA were analyzed by ethidium bromide staining.
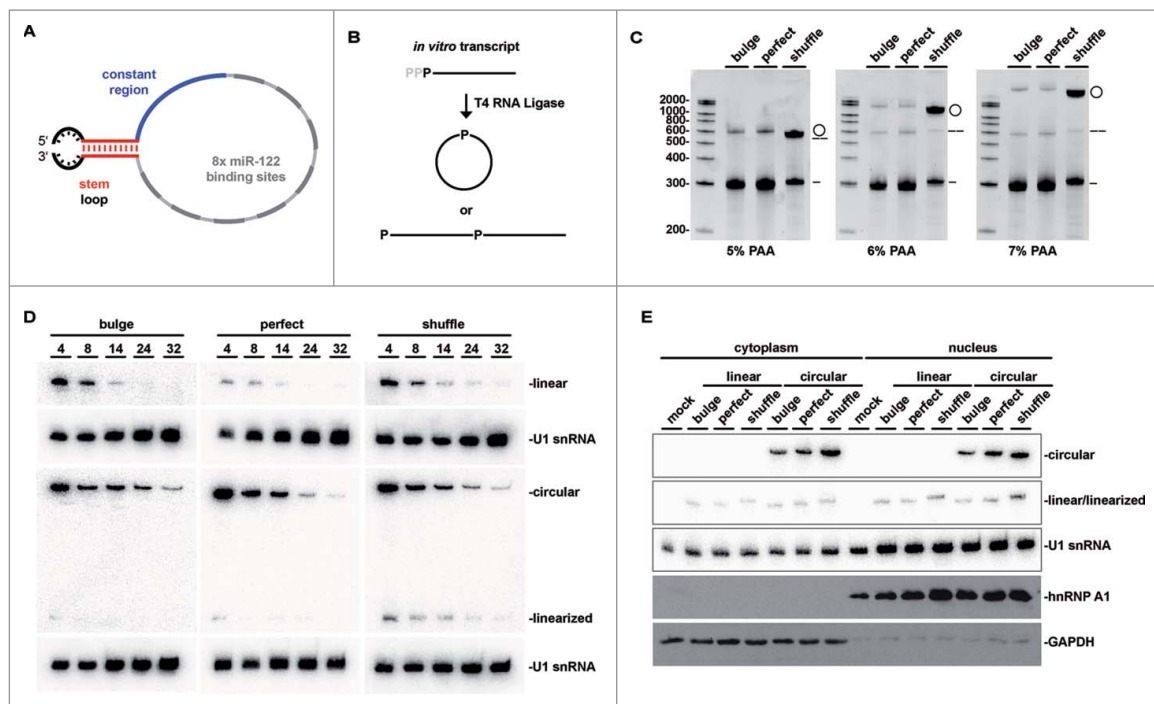
Figure 2. Preparation and analysis on circular RNA *in vitro*. (A) Schematic of *in vitro* circularization constructs. Transcripts to be circularized consist of a terminal 10 nt open loop structure (black) and a reverse-complementary repeat sequence of 11 nt, which forms an intramolecular stem (red). This structure is followed by a 63 nt constant region for detection by northern blot or PCR (blue), followed by the miRNA-122 sponge (bulge; perfect) or a scrambled control sequence (shuffle) in grey. (B) Schematic of the *in vitro* ligation reaction. 4-fold excess of GMP over GTP results in ~80% of the transcripts containing a 5′-monophosphate, enabling efficient *in vitro* ligation by T4 RNA ligase. Ligation products are circular RNAs (intramolecular ligation) or linear dimers (intermolecular ligation). (C) *In vitro* ligation reactions described in (B) were analyzed on 5%, 6% or 7% polyacrylamide-urea gels by ethidium bromide staining. While mobility of linear RNAs remains unchanged compared to RNA marker, the apparent mobility of circular RNA is lower in higher percentage gels (indicated by dash/double dash or circle). (D) Purified linear or circular RNAs from (C) were transfected in HuH-7.5 cells and total RNA was prepared after 4, 8, 14, 24 and 32 h. RNAs were detected by ^{32}P-northern blot analysis using identical probes in the constant region [labeled blue in (A)]. (E) HuH-7.5 cells transfected with circular RNA or linear RNA from (C) were subjected to sub-cellular fractionation and cytoplasmic or nuclear fractions were analyzed by ^{32}P-northern blot detecting transfected RNAs along with U1 snRNA and by western blot against hnRNP A1 or GAPDH proteins as a fractionation control. In the circRNA-transfected samples, a degradation product is detected at linear monomer size ("linearized").

UTRs used in Fig. 1 did not circularize efficiently, a shuffled control sequence that does not bind miRNA-122 was used (Fig. S1B, C). The differences in circularization efficiency between repetitive sponge sequences (bulge, perfectly complementary) and the shuffled control sequence is most likely due to secondary structure effects. Circular RNAs and their linear counterparts were gel-purified and circularity was verified using differential retardation in polyacrylamide gels (Fig. S2A), RNase R exonuclease treatment (Fig. S2B) and Sanger sequencing (Fig. S2C-E). When transfected into HuH-7.5 cells in equal amounts by liposomes and analyzed by northern blot after 4 to 32 hours, the circular RNAs appear not to be more stable than their linear counterparts under these conditions (Fig. 2D, Fig. S3A: circRNA $t_{1/2}$: 6.9 to 9.4 h; linear RNA $t_{1/2}$: 5.7 to 8.3 h). We believe that liposomes have an influence on evaluation of the RNA stability since they could result in differential uptake of circular versus linear RNAs, protect RNAs from degradation outside of the cell, withhold or continuously release RNA into the cell. To omit these technical errors, we used electroporation to measure the intracellular stability of the circular versus the linear RNA sponges (Fig. S3B, C). Importantly, the circular RNAs are first cleaved to a linear form that is in turn subjected to decay. Considering the available miRNA-122 binding sites in the cell, the amount of circular and linearized molecules has to be added up. We determined half-life times of 11.3-13.2 h for

the linear RNAs, and 14.1-19.1 h for the circular form, whereas the total half-life of the circular RNA sponge in the cell is 18.7-22.7 h (Fig. S3C).

It has been reported that endogenous circRNAs mainly localize to the cytoplasm [1,2,4,5], but the transfected *in vitro* produced circRNAs can be found in the nucleus as well as in the cytoplasm in comparable amounts (Fig. 2E). This finding qualifies *in vitro* generated circRNAs to be used as a potent molecular tool, since also nuclear events like chromatin re-modeling, transcription or pre-mRNA splicing could be altered using circRNAs.

Although the competing endogenous RNA (ceRNA)-hypothesis has been controversially discussed [20,21], exogenously synthesized linear miRNA decoys have been successfully used before. An outstanding example of a functioning anti-miRNA drug is Miravirsen. The LNA/DNA mixmer reduced virus titers of patients injected subcutaneously over four weeks to non-detectable levels [12]. A disadvantage of LNA-containing anti-miRNA drugs is their potential accumulation of unmetabolizable LNA nucleotides in the patient and their hepatotoxic effect in animal models, which is linked to the LNA modification rather than to down-regulation of its target [22].

CircRNAs are more stable than their linear counterparts (see Fig. 2D, Fig. S3 and [2,5]), but not indefinitely stable and most probably enter standard recycling pathways as

any RNA molecule in the cell, which may not be the case for Miravirsen. To analyze if the artificial circular RNA sponges can fulfill a similar function as an anti-miRNA drug, two different HCV-reporter systems were utilized. First, we used a non-infectious HCV/luciferase reporter system, where the major part of the HCV polyprotein open reading frame (ORF) is substituted by a luciferase ORF (Fig. 3A) [9]. The natural start codon and first 33 nt of the Core protein coding sequence were retained, maintaining the structure of the internal ribosome entry site. Transfection of both the bulged and the perfectly complementary miRNA-122 binding site-containing linear and circular RNAs or Miravirsen oligonucleotide significantly reduced luciferase activity, while the shuffled sequence-containing RNAs did not (Fig. 3B). Stability of the reporter RNA was not affected by the transfections of the RNA sponges or Miravirsen under these conditions, arguing for an exclusive translational repression effect of miRNA-122 sequestration in this system (Fig. S4A, B).

Ultimately, the *in vitro* produced circRNAs were compared with the Miravirsen anti-miRNA oligonucleotide in an infectious, wildtype HCV system. We co-transfected HuH-7.5 cells with full-length Jc1 HCV RNA and either Miravirsen antisense oligonucleotide or similar amounts of linear or circular RNA. The HCV Jc1 construct is a full-length replication-competent chimeric clone capable of autonomous replication and yields high infectious titers in HuH-7.5 cells [23]. Linear as well as circular RNA sponges were still detectable using the high-sensitive Digoxigenin-detection northern blot five days post-transfection (Fig. 3C). It is important to mention that similar absolute mass quantities of circRNAs and Miravirsen were transfected, which represents a three-fold higher molarity of miRNA-122 binding sites in the Miravirsen experiment.

Co-transfection of linear or circular miRNA-122 sponges with HCV RNA reduced viral NS3 and Core intracellular protein levels to almost undetectable levels five days post-transfection similarly as the Miravirsen oligonucleotide (Fig. 3D). Both linear and circular shuffled control RNAs did not affect HCV protein levels. When transfecting limiting amounts of miRNA-122 sponges (one fifth in comparison to Fig. 3D), it becomes apparent that the circular molecules have a more pronounced effect on viral protein production (Fig. S4C). The circular RNA that contains the
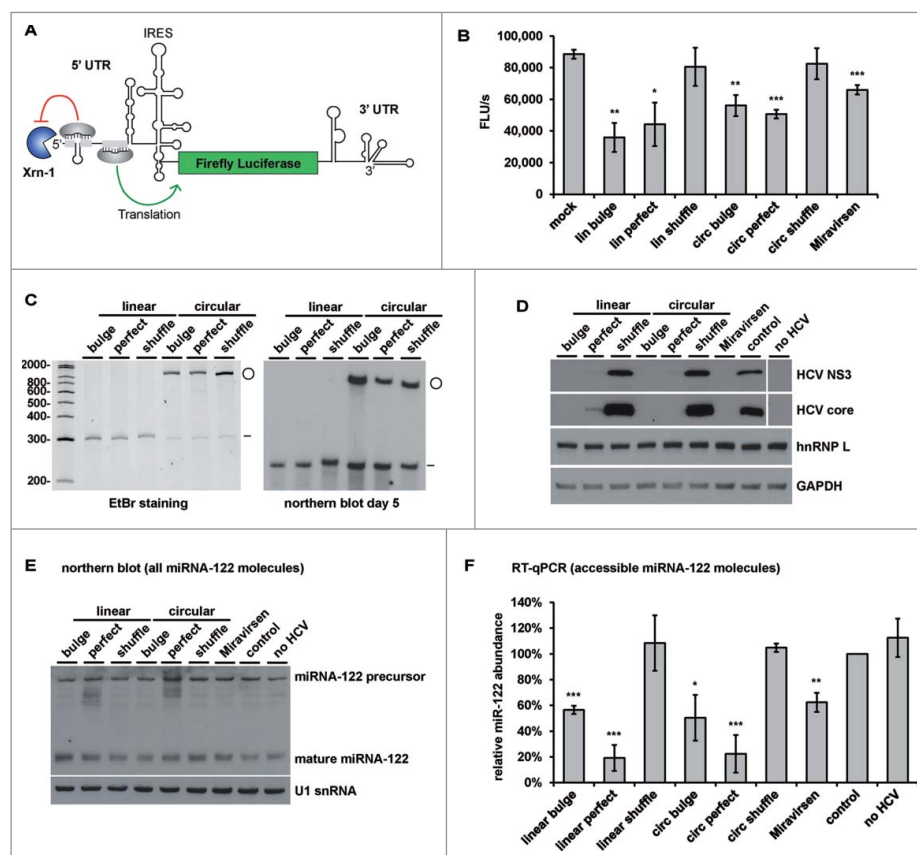

Figure 3. Circular miRNA-122 RNA sponges affect HCV translation. (A) Schematic of the HCV/luciferase reporter construct. The HCV polyprotein open reading frame (ORF) was replaced by a firefly luciferase gene, leaving the original start codon and part of the Core protein ORF intact due to IRES secondary structure elements present in the region. miRNA-122 binding sites 1 and 2 are depicted, with Ago/miRNA bound and indicate its function in protection from Xrn-1-mediated degradation and in translation stimulation. (B) Linear and circular RNAs shown in Fig. 2C or Miravirsen were transfected one day prior to the reporter construct shown in (A). Luciferase activity of the reporter was measured 4 h post-transfection and normalized to reporter-only transfection ("mock"). Error bars represent s.d. (n = 3) $^*P < 0.05$; $^{**}P < 0.01$; $^{***}P < 0.001$. (C) Ethidium bromide staining (left panel) of RNA prior to co-transfection into HuH-7.5 cells together with full-length HCV RNA (strain Jc1), and same RNAs detected via northern blot 5 days post-transfection (right panel). (D) Western blot of cell lysates from HuH-7.5 cells co-transfected with full-length HCV RNA and linear/circular RNAs from (C) or Miravirsen LNA/DNA mixmer oligonucleotide 5 days post-transfection. Equal amounts of total protein was loaded. Viral NS3 and Core, and cellular hnRNP L and GAPDH proteins were detected. (E,F) Total RNA from the same cells as in (D) was isolated, and steady-state miRNA-122 levels and U1 snRNA were detected via northern blot (E) and TaqMan-RT-qPCR [normalized to miRNA-22 and control (mock) transfection, (F)]. Error bars represent s.d. (n = 3) $^*P < 0.05$; $^{**}P < 0.01$; $^{***}P < 0.001$.

bulged miRNA-122 binding site reduces levels of both viral proteins more efficiently then Miravirsen under these conditions.

It has been reported that highly complementary miRNA binding sites can trigger tailing and trimming and thereby destabilization of miRNAs [24,25]. Therefore we tested steady-state miRNA-122 level by northern blot. Neither the precursor, nor the mature miRNA-122 were altered by any of the treatments (Fig. 3E).

Northern blot detects all miRNA-122 molecules in the cell, including those sequestered by sponges, whereas reverse transcription and TaqMan qPCR detects only functionally available miRNA-122 (Fig. 3F). This hypothesis was tested by splitting the total RNA prepared from cells transfected with circRNA sponges. One half was mixed with reverse transcription primers and denatured prior to reverse transcription. This led to release of miRNA-122 from the sponges, annealing of primers, and detection of unaltered miRNA-122 levels (Fig. S4D). Therefore, the decrease of miRNA-122 levels in the experiments where molecular sponges were transfected demonstrates functional sequestration. Similar effects on miRNA levels detected by RT-qPCR were recently reported for sequestration of miRNA-17 and -221 by small RNA zippers [26].

In this study we designed artificial *in vitro* transcribed and ligated circRNA sponges that sequester miRNA-122 from HCV in a manner similar to Miravirsen, an LNA-modified antisense oligonucleotide. Furthermore, circular RNAs could not only be used as miRNA sponges, but might also work as protein sponges using binding sites derived from SELEX- or CLIP-data available for many RNA-binding proteins. A circular miRNA-122 RNA sponge against HCV could be combined with sequences that sequester host factors necessary for HCV propagation, such as hnRNP L [27], HuR and the La protein [28], or even viral proteins themselves. RNA aptamers against NS3 and NS5B have been used to inhibit HCV replication [29], and can easily be included in circular RNAs. Although not many other viruses are known to hijack host miRNAs yet, a recent study found that the bovine viral diarrhea virus (BVDV) is dependent on miRNA-17 and let-7 [30], a potential additional target for antiviral circRNA sponges. In the future, approaches like this will certainly require other, large-scale methods for circRNA production than *in vitro* ligation. It has been shown that circular RNA can also be produced by alternative methods, e.g. by expression in bacteria using constructs containing permutated group I introns [31] or by the tRNA splicing mechanism [32]. Nonetheless, both circRNAs synthesized *in vitro* as well as potential plasmid-based expression constructs that produce artificial circRNAs *in vivo* require transport into the cell by an adequate delivery platform. As summarized in [33], lipid nanoparticles (LNPs) and synthetic nanoparticles are currently still the best choice to overcome cellular barriers for RNA therapeutics. Taken together, artificial circRNA sponges are a promising tool in molecular medicine and biology with a wide range of potential applications.

Materials and methods

Cell culture and transfections

HuH-7 and HuH-7.5 cells [34] were cultured in DME-medium supplemented with 10% FBS (Gibco), GlutaMAX (Gibco) and non-essential amino acids (Sigma) at 37°C and 5% CO_2. Cells were transfected using Lipofectamine 2000 (Thermo Fisher Scientific) according to the manufacturer's instructions, or by electroporation using GenePulser Xcell (Bio-Rad). For the latter, cells were trypsinized, pelleted by centrifugation at 1500 rpm, rinsed with PBS and reconstituted in Cytomix (120 mM KCl, 0.15 mM $CaCl_2$, 10 mM K_2HPO_4/KH_2PO_4 (pH 7.6), 25 mM Hepes, 2 mM EGTA, 5 mM $MgCl_2$, pH is adjusted to 7.6 with KOH; supplemented by 2 mM ATP and 5 mM glutathione before use) to 10^7 cells/ml. Electroporation was performed with 400 μl cell suspension in 4 mm cuvettes (Sigma) with the following settings: square wave, 270 V, 20 ms, single pulse.

MicroRNA binding site luciferase reporter assays

Luciferase reporter assays were performed using the pmirGLO dual-luciferase miRNA target expression vector system (Promega). Four copies the miRNA-122 binding site sponge sequences or controls (Fig. 1A) were cloned into the firefly luciferase reporter 3′-UTR. Four nucleotides spacing in between single sites (AGCC) result in optimal spacing between seed sites to allow efficient binding of multiple miRNA/Ago2 complexes [18]. As negative controls, fragments of unrelated 3′-UTRs (KPNB1, HNRNPK, and LAPTM4A) were cloned into the firefly reporter 3′-UTR. Three wells of a 12-well dish of HuH-7.5 cells were transfected with 500 ng plasmid per well as replicates. After 16 h of expression, luciferase activity was measured using beetle juice and renilla juice (PJK) by a Centro LB 960 Microplate Luminometer (Berthold). The firefly luciferase activity was normalized to renilla luciferase activity and adjusted to LAPTM4A. Standard deviations were calculated for the biological triplicates.

For RT-PCR, HuH-7.5 cells were seeded on 6 cm dishes and transfected with 5 μg of the reporter plasmids. Cells were harvested 2 days post-transfection, RNA was isolated using Trizol reagent (Thermo Fisher Scientific) and the RNeasy kit (Qiagen). To eliminate plasmid DNA contamination, samples were additionally treated with RQ1 DNase (Promega). 500 ng of total RNA was subjected to reverse transcription using the qScript cDNA Synthesis Kit (Quanta Biosciences). PCR was performed using specific primers for GAPDH mRNA (fwd: tgcaccaccaactgcttagc, rev: ggcatggactgtggtcatgag), renilla mRNA (fwd: aactggagcctgaggagttc, rev: tagctccctcgacaatagcg) and primers flanking the miRNA-122 binding site insertion in the firefly reporter 3′-UTR (fwd: ccaagaagggcggcaagat, rev: gccaactcagcttcctttcg). After 23 cycles of PCR the products were separated by 2% agarose gel electrophoresis and analyzed by ethidium bromide staining.

Neutravidin-Biotin in vitro pulldown assays

In vitro transcription was performed using the HiScribe T7 High Yield RNA Synthesis Kit (NEB) and 3′-end biotinylated as described in [35]. Neutravidin agarose beads (Thermo Fisher Scientific) were blocked overnight with tRNA, BSA and glycogen and incubated with 800 fmol of chemically 3′-end biotinylated *in vitro* transcripts for 30 min. After washing with 600 mM KCl (20 mM HEPES pH 7.5), beads were incubated with extracts from HuH-7 or HuH-7.5 cells that were lysed using RIPA buffer for 1 h at 37°C. After extensive washing with

600 mM KCl, bead-bound RNA was isolated using Trizol reagent. RNA was analyzed by ethidium bromide staining to visualize bound transcripts, or by northern blot using EDC crosslinking [36] and ^{32}P-labeled DNA oligonucleotides or Digoxigenin-LNA-probes (Exiqon) to visualize bound miRNA-122 via autoradiography or the DIG-detection system (Roche).

Design and transcription of in vitro circularization constructs

8-mers of miRNA-122 sponges were constructed from two *in vitro* ligated dsDNA tetramers (ordered from Sigma, 4 bp spacing, flanked by *Nhe*I and *Xba*I restriction sites) and placing into a circularization backbone that had been cloned into pCR2.1-vector before. The shuffled sequence was generated by using a sequence randomizer ("shuffle DNA", [37]) on an array of endogenous miRNA-122 binding sites (data not shown), and produced by gene synthesis with flanking *Nhe*I and *Xba*I restriction sites and cloned in the same way. The circularization backbone contains sequences that favor *in vitro* circularization of a corresponding transcript (see also Fig. 2A). It contains a T7 promoter, the first half of an open loop (5 nt starting with the GGG of every T7 RNA polymerase transcript), and 11 nt that form a stem with the end of the transcript. This stem is followed by a 63 nt constant region that is similar for all circRNA constructs and serves as a platform for northern probes and PCR primers. The actual miRNA-122 sponge (8-mer, see above) is then flanked by the second half of the 11 nt stem and another 5 nt of an open loop. The transcript's 3'-end is created by *Eco*RI cleavage that also produces the 3'-end of the template for T7 RNA polymerase transcription. Construct sequences are represented in Fig. S5.

In vitro transcription was performed using the HiScribe T7 High Yield RNA Synthesis Kit in presence of a 4-molar excess of GMP (final concentration of 40 mM, Sigma) to produce ~80% monophosphate 5'-ends, which are required as a substrate for T4 RNA ligase in the *in vitro* circularization reaction. DNA template was digested by RQ1 DNase and free nucleotides were removed by gel filtration using mini Quick Spin RNA Columns (Roche).

In vitro circularization and RNA purification

The circularization protocol is a modified version of the protocol described in [38]. The transcripts were denatured at 95°C in the presence of 50 mM NaCl, and then slowly cooled to 25°C (1°C every 10 s) to resolve secondary structures and facilitate annealing of the terminal stem loop structure for *in vitro* circularization. Next, T4 RNA ligase buffer and RNaseOUT (Thermo Fisher Scientific) were added and incubated for 10 min at 37°C. To facilitate *in vitro* circularization, ATP is added to 200 nM, DMSO to 15% (v/v) and T4 RNA ligase 1 to 0.2 U/μl and the reaction is incubated in 250 μl for 16 h at 16°C. Ligations were analyzed on denaturing 5%, 6% and 7% polyacrylamide-urea gels to distinguish circular RNA from linear dimers. Circular and linear monomers were then purified from a preparative denaturing 7% polyacrylamide-urea gel via UV-shadowing and gel elution in 800 μl PK-buffer containing 1% SDS for 1 h at 50°C. RNA was extracted using phenol extraction and ethanol precipitation and analyzed on denaturing polyacrylamide-urea gels as described above.

RNase R treatment

100 ng of circular or linear gel-purified RNA was incubated with or without 1.5 U RNase R (Epicentre) in a reaction volume of 10 μl for 30 min at 37°C. 50% of the reactions were loaded on a 7% denaturing polyacrylamide gel and RNAs were visualized by ethidium bromide staining.

Stability assay

HuH-7.5 cells were seeded on 6-well plates and transfected with 100 ng of circular or linear RNA per well using Lipofectamine 2000. After 4 hours cells were washed with PBS and medium was exchanged. Cells were harvested using Trizol at time points 4, 8, 14, 24 and 32 h after transfection, followed by RNA extraction. 20% of each sample was subjected to 7% denaturing polyacrylamide gel electrophoresis and northern blot (see below). Alternatively, for the stability assay using electroporation, 4×10^6 HuH-7.5 cells were transfected with 600 ng of circular or linear RNA as described above. Transfected cells were seeded onto 6-well plates (2 ml per well); input samples were directly harvested (time point 0). The medium exchange was performed 8 h post electroporation; cells were lysed by Trizol at time points 8, 24, 48, 72 h, followed by total RNA isolation. 20% of each sample was subjected to 7% denaturing polyacrylamide gel electrophoresis and northern blot (see below).

Subcellular fractionation

HuH-7.5 cells were seeded on 6 cm dishes and transfected with 3 μg of circular or linear RNA using Lipofectamine 2000. After 16 h, cells were harvested, samples were adjusted to the cell count and subjected to subcellular fractionation using the NE-PER Nuclear and Cytoplasmic Extraction kit (Thermo Fisher Scientific). 75% of the nuclear and cytoplasmic extracts were used for RNA preparation. Transfected RNAs and U1 snRNA were detected by northern blot (see below). 15% of the lysates were subjected to western blot, detecting hnRNP A1 (monoclonal antibody 4B10, Santa Cruz Biotechnology) and GAPDH (monoclonal antibody GAPDH-71.1, Sigma).

Cloning and sequencing of circRNAs

After 5 days of transfection in HuH-7.5 cells as described above, total RNA was isolated using Trizol reagent and 1 μg of total RNA was reverse transcribed using qScript cDNA Synthesis Kit and amplified by PCR (25 cycles) using outfacing primers in the constant regions specific for circular RNAs as indicated in Fig. S2C. PCR products were cloned (TOPO-TA cloning, Thermo Fisher Scientific) and Sanger sequenced.

HCV-UTR/Luciferase assay

Transcription templates were generated via PCR using primers at the end of the 5'- and 3'-UTR, respectively (fwd: aattaatacgactcac-tatagccag, rev: acatgatctgcagagaggcc) and the plasmid pHCV-374-

Fluc-3′-UTR [39]. 1 μg of gel-purified template was *in vitro* transcribed with the HiScribe T7 High Yield RNA Synthesis Kit in a 50 μl volume for 1.5 h at 37°C. The template was digested using RQ1 DNase and purified using mini Quick Spin RNA Columns, followed by phenol/chloroform extraction and ethanol precipitation. RNA quality was analyzed by denaturing 1.2% agarose gel electrophoresis. HuH-7.5 cells were seeded in a 12-well plate the day before the first transfection, and 200 ng/well (Fig. 3B) or 150 ng/well (Fig. S1B, C) of circular RNA, linear RNA or Miravirsen were transfected using Lipofectamine 2000. Medium was changed after 16 h, 1 h prior to the second transfection of 150 ng of HCV-UTR/Luciferase reporter RNA per well. 4 h after reporter transfection cells were lysed and firefly luciferase activity was measured as described above. Three wells were transfected per condition to determine the mean luciferase activity and standard deviations. A one sided t test for unequal variances was performed to determine the level of significance compared to mock transfection. In a similar setup, cells were lysed using Trizol reagent, total RNA was prepared and RT-PCR was performed to monitor reporter RNA stability using primers targeting the HCV 5′-UTR (fwd: tgagcacgaatcctaaacctc, rev: tgagcacgaatcctaaacctc).

Full-length wildtype HCV experiments

The ability of the RNA sponges to sequester miRNA-122 was compared to that of a Miravirsen LNA/DNA mixmer oligonucleotide (Exiqon) in the full-length HCV infection system. Therefore, HuH-7.5 cells were co-transfected with Jc1 chimeric HCV RNA genomes [21] and circular or linear RNA monomers or Miravirsen oligonucleotide using Lipofectamine 2000 reagent. The Jc1 RNA transcripts were generated by *in vitro* transcription using T7 RNA Polymerase (NEB) from *Mlu*I-cut plasmid pFK-JFH1-J6 C-846_dg (Jc1). For transfections, 933 ng (0.3 pmol) of Jc1 RNA and 200 ng of RNA sponges or Miravirsen were applied to HuH-7.5 cells in 6-well plates in duplicates; the controls of HCV infection and non-infected cells were carried out therewith. In the experiments with limiting RNA sponge, 0.1 pmol of Jc1 RNA was co-transfected with 10 ng of RNA sponges into HuH-7.5 cells in 12-well plates. 5 days after transfection total RNA and cell lysates were isolated for downstream analyses. Isolation of total RNA was performed as described above.

HCV protein expression was evaluated by western blot analysis of equal total protein amounts using antibodies against HCV Core (monoclonal antibody C7-50, Thermo Fisher Scientific) and NS3 (monoclonal antibody 8G-2, Abcam) proteins along with the cellular hnRNP L (monoclonal antibody 4D11, Sigma) and GAPDH (monoclonal antibody GAPDH-71.1, Sigma) as reference proteins.

CircRNA detection by northern blot

For detection of circular and linear RNAs, total RNA was separated on a 6% or 7% denaturing polyacrylamide gel, transferred to a nylon membrane and hybridized at 65°C with either digoxigenin- labelled or ^{32}P-internally labelled 73 nt riboprobes directed against the constant region of the linear and circular RNAs. For the experiments shown in Fig. 2F and 2G a mixture of ^{32}P-labelled probes for the constant region of the circRNAs

and U1 snRNA was used (20 ng/ml each). DIG-northern blots were developed using the DIG-detection system and ^{32}P-northern blots were visualized by phosphorimaging and the Typhoon FLA 9500 (GE). Quantification of bands intensity was conducted using ImageQuantTL software, and normalized to 4 h values (for the experiment in Fig. 2D and Fig. S3A) or to 8 h (for the experiment in Fig. S3B,C). Half-life values for circRNA variants and their counterparts were derived by fitting to exponential decay function using OriginPro8 software (ExpDec1 function: y = A1* exp(-x/t)+y0).

miRNA detection

miRNA-122 steady-state levels in HCV-transfected HuH-7.5 cells were determined by northern blot as described above for the Neutravidin-biotin *in vitro* pulldown assay. 6 μg of total RNA 5 days post-transfection was loaded. Detection of miRNA-122 levels by RT-qPCR was performed using the TaqMan microRNA detection system (Thermo Fisher Scientific), using 75 ng of total RNA in the miRNA-122 assay or miRNA-22 assay for normalization using the Pfaffl method of qPCR analysis [40]. Denaturing conditions in TaqMan RT-qPCR were artificially recreated by heating total RNA samples with primers at 95°C for 2 min followed by cooling on ice, and subsequent enzyme supplementation.

Disclosure of potential conflicts of interest

No potential conflicts of interest were disclosed.

ORCID

Albrecht Bindereif 🆔 http://orcid.org/0000-0002-7730-7380

References

[1] Salzman J, Gawad C, Wang PL, et al. Circular RNAs are the predominant transcript isoform from hundreds of human genes in diverse cell types. PLoS One. 2012;7(2):e30733. doi:10.1371/journal.pone.0030733

[2] Jeck WR, Sorrentino JA, Wang K, et al. Circular RNAs are abundant, conserved, and associated with ALU repeats. RNA. 2013;19(2):141–57. doi:10.1261/rna.035667.112

[3] Chen LL. The biogenesis and emerging roles of circular RNAs. Nat Rev Mol Cell Biol. 2016;17(4):205–11. doi:10.1038/nrm.2015.32

[4] Hansen TB, Jensen TI, Clausen BH, et al. Natural RNA circles function as efficient microRNA sponges. Nature. 2013;495(7441):384–8. doi:10.1038/nature11993

[5] Memczak S, Jens M, Elefsinioti A, et al. Circular RNAs are a large class of animal RNAs with regulatory potency. Nature. 2013;495(7441):333–8. doi:10.1038/nature11928

[6] Piwecka M, Glažar P, Hernandez-Miranda LR, et al. Loss of a mammalian circular RNA locus causes miRNA deregulation and affects brain function. Science. 2017;357(6357):pii: eaam8526. doi:10.1126/science.aam8526

[7] Sarnow P, Sagan SM. Unraveling the Mysterious Interactions Between Hepatitis C Virus RNA and Liver-Specific MicroRNA-122. Annu Rev Virol. 2016;3(1):309–332. doi:10.1146/annurev-virology-110615-042409

[8] Li Y, Masaki T, Yamane D, et al. Competing and noncompeting activities of miR-122 and the 5′ exonuclease Xrn1 in regulation of hepatitis C virus replication. Proc Natl Acad Sci U S A. 2013;110(5):1881–6. doi:10.1073/pnas.1213515110

[9] Henke JI, Goergen D, Zheng J, et al. microRNA-122 stimulates translation of hepatitis C virus RNA. EMBO J. 2008;27(24):3300–10. doi:10.1038/emboj.2008.244

[10] Machlin ES, Sarnow P, Sagan SM. Masking the 5′ terminal nucleotides of the hepatitis C virus genome by an unconventional microRNA-target RNA complex. Proc Natl Acad Sci U S A. 2011;108(8):3193–8. doi:10.1073/pnas.1012464108

[11] Nieder-Röhrmann A, Dünnes N, Gerresheim GK, et al. Cooperative enhancement of translation by two adjacent microRNA-122/Argonaute 2 complexes binding to the 5untranslated region of Hepatitis C Virus RNA. J Gen Virol. .2017;98(2):212–224. doi:10.1099/jgv.0.000697

[12] Janssen HL, Reesink HW, Lawitz EJ, et al. Treatment of HCV infection by targeting microRNA. N Engl J Med. 2013;368(18):1685–94. doi:10.1056/NEJMoa1209026

[13] Hildebrandt-Eriksen ES, Aarup V, Persson R, et al. A locked nucleic acid oligonucleotide targeting microRNA 122 is well-tolerated in cynomolgus monkeys. Nucleic Acid Ther. 2012;22(3):152–61. doi:10.1089/nat.2011.0332

[14] van der Ree MH, de Vree JM, Stelma F, et al. Safety, tolerability, and antiviral effect of RG-101 in patients with chronic hepatitis C: a phase 1B, double-blind, randomised controlled trial. Lancet. 2017;389(10070):709–717. doi:10.1016/S0140-6736(16)31715-9

[15] Wang B, Wang H, Yang Z. MiR-122 inhibits cell proliferation and tumorigenesis of breast cancer by targeting IGF1R. PLoS One. 2012;7(10):e47053. doi:10.1371/journal.pone.0047053

[16] Jinek M, Doudna JA. A three-dimensional view of the molecular machinery of RNA interference. Nature. 2009;457(7228):405–12. doi:10.1038/nature07755

[17] Schirle NT, Sheu-Gruttadauria J, MacRae IJ. Structural basis for microRNA targeting. Science. 2014;346(6209):608–13. doi:10.1126/science.1258040

[18] Saetrom P, Heale BS, Snøve O Jr, et al. Distance constraints between microRNA target sites dictate efficacy and cooperativity. Nucleic Acids Res. 2007;35(7):2333–42. doi:10.1093/nar/gkm133

[19] Tabak HF, Van der Horst G, Smit J, et al. Discrimination between RNA circles, interlocked RNA circles and lariats using two-dimensional polyacrylamide gel electrophoresis. Nucleic Acids Res. 1988;16(14A):6597–605. doi:10.1093/nar/16.14.6597

[20] Denzler R, Agarwal V, Stefano J, et al. Assessing the ceRNA hypothesis with quantitative measurements of miRNA and target abundance. Mol Cell .2014;54(5):766–76. doi:10.1016/j.molcel.2014.03.045

[21] Jens M, Rajewsky N. Competition between target sites of regulators shapes post-transcriptional gene regulation. Nat Rev Genet. 2015;16(2):113–26. doi:10.1038/nrg3853

[22] Swayze EE, Siwkowski AM, Wancewicz EV, et al. Antisense oligonucleotides containing locked nucleic acid improve potency but cause significant hepatotoxicity in animals. Nucleic Acids Res. 2007;35(2):687–700. doi:10.1093/nar/gkl1071

[23] Pietschmann T, Kaul A, Koutsoudakis G, et al. Construction and characterization of infectious intragenotypic and intergenotypic hepatitis C virus chimeras. Proc Natl Acad Sci U S A. 2006;103(19):7408–13. doi:10.1073/pnas.0504877103

[24] Ameres SL, Horwich MD, Hung JH, et al. Target RNA-directed trimming and tailing of small silencing RNAs. Science. 2010;328(5985):1534–9. doi:10.1126/science.1187058

[25] de la Mata M, Gaidatzis D, Vitanescu M, et al. Potent degradation of neuronal miRNAs induced by highly complementary targets. EMBO Rep. 2015;16(4):500–11. doi:10.15252/embr.201540078

[26] Meng L, Liu C, Lü J, et al. Small RNA zippers lock miRNA molecules and block miRNA function in mammalian cells. Nat Commun. 2017;8:13964. doi:10.1038/ncomms13964

[27] Hwang B, Lim JH, Hahm B, et al. hnRNP L is required for the translation mediated by HCV IRES. Biochem Biophys Res Commun. 2009;378(3):584–8. doi:10.1016/j.bbrc.2008.11.091

[28] Shwetha S, Kumar A, Mullick R, et al. HuR Displaces Polypyrimidine Tract Binding Protein To Facilitate La Binding to the 3′ Untranslated Region and Enhances Hepatitis C Virus Replication. J Virol. 2015;89(22):11356–71. doi:10.1128/JVI.01714-15

[29] Lee CH, Lee YJ, Kim JH, et al. Inhibition of hepatitis C virus (HCV) replication by specific RNA aptamers against HCV NS5B RNA replicase. J Virol. 2013;87(12):7064–74. doi:10.1128/JVI.00405-13

[30] Scheel TK, Luna JM, Liniger M, et al. A Broad RNA Virus Survey Reveals Both miRNA Dependence and Functional Sequestration. Cell Host Microbe. 2016;19(3):409–23. doi:10.1016/j.chom.2016.02.007

[31] Umekage S, Kikuchi Y. In vitro and in vivo production and purification of circular RNA aptamer. J Biotechnol. 2009;139(4):265–72. doi:10.1016/j.jbiotec.2008.12.012

[32] Schmidt CA, Noto JJ, Filonov GS, et al. A Method for Expressing and Imaging Abundant, Stable, Circular RNAs In Vivo Using tRNA Splicing. Methods Enzymol. 2016;572:215–36. doi:10.1016/bs.mie.2016.02.018

[33] Dowdy SF. Overcoming cellular barriers for RNA therapeutics. Nat Biotechnol. 2017;35(3):222–229. doi:10.1016/bs.mie.2016.02.018

[34] Blight KJ, McKeating JA, Rice CM. Highly permissive cell lines for subgenomic and genomic hepatitis C virus RNA replication. J Virol. 2002;76(24):13001–14. doi:10.1128/JVI.76.24.13001-13014.2002

[35] Willkomm DK, Hartmann RK. 3′-Terminal Attachment of Fluorescent Dyes and Biotin. In: Handbook of RNA Biochemistry: Second Edition. Weinheim (Germany): Wiley-VCH; 2014; p. 117–128.

[36] Kim SW, Li Z, Moore PS, et al. A sensitive non-radioactive northern blot method to detect small RNAs. Nucleic Acids Res. 2010;38(7):e98. doi:10.1093/nar/gkp1235

[37] Stothard P. The Sequence Manipulation Suite: JavaScript programs for analyzing and formatting protein and DNA sequences. Biotechniques. 2000;28:1102–1104.

[38] Pan T. Probing RNA structure and function, by circular permutation. Methods Enzymol. 2000;317:313–30. doi:10.1016/S0076-6879(00)17022-3.

[39] Conrad KD, Giering F, Erfurth C, et al. MicroRNA-122 dependent binding of Ago2 protein to hepatitis C virus RNA is associated with enhanced RNA stability and translation stimulation. PLoS One. 2013;8(2):e56272. doi:10.1371/journal.pone.0056272

[40] Pfaffl MW. A new mathematical model for relative quantification in real-time RT-PCR. Nucleic Acids Res. 2001 May 1;29(9):e45. doi:10.1093/nar/29.9.e45